THE JOURNAL OF PHYSICAL CHEMISTRY A

pubs.acs.org/JPCA Article

# Temperature and Nuclear Quantum Effects on the Stretching Modes of the Water Hexamer

Nagaprasad Reddy Samala and Noam Agmon*

Cite This: *J. Phys. Chem. A* 2020, 124, 8201−8208 Read Online

ACCESS | Metrics & More | Article Recommendations | Supporting Information

**ABSTRACT:** The water hexamer has many low-lying isomers, e.g., ring, book, cage, and prism, shifting from two- to three-dimensional structures. We show that this dimensionality change is accompanied by a drop in the quantum nature of the cluster, as manifested in the red shift of the quantal OH stretching modes as compared with their classical counterparts. We obtain this "nuclear quantum effect" (NQE) as the mean deviation between the OH stretch frequencies from velocity autocorrelation Fourier transforms from classical trajectories on a high-level water potential (MB-pol) as compared with scaled harmonic frequencies from high-level quantum chemistry calculations. With a universal scaling factor, the predicted OH frequencies agree with experiment to a mean absolute deviation $\lesssim$10 cm$^{-1}$, which allows unequivocal isomer assignments. By assuming temperature-independent NQEs, we produce the temperature dependence of the cage isomer OH stretch spectrum below 70 K, where it is the dominant structure. All bands widen and blue-shift with increasing temperature, most conspicuously the reddest mode, which thus constitutes a "vibrational thermometer".

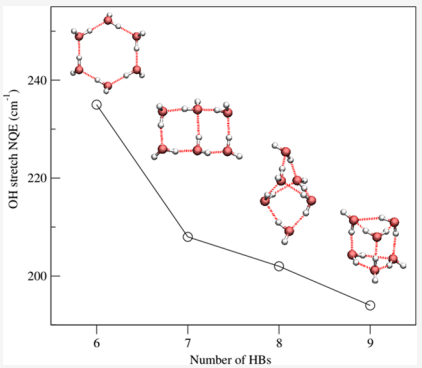


## INTRODUCTION

The water hexamer, $W_6 \equiv (H_2O)_6$, has a plethora of hydrogen-bonded (HBed) isomers, with similar energies and illustrative names, such as book, cage, ring, and prism (Figure 1).[1] The book is a ring with one additional HB across its center, which therefore looks like two tetramers sharing a common dimer (i.e., a rectangle composed of two squares). The cage has an additional HB between two water molecules on the main diagonal of the rectangle, rendering it the smallest isomer with three-dimensional (3D) structure. Finally, the prism can be envisioned as a book isomer in which two HBs were added between adjacent corners of the rectangle. Thus, the number of HBs increases systematically in this series: 6 (ring), 7 (book), 8 (cage), and 9 (prism).

The best theoretical estimates for the total dissociation energies (in kcal/mol) increase monotonically with the number of HBs: 44.3 (ring), 45.4 (book), 45.9 (cage), and 46.2 (prism).[2] Nevertheless, the cage (rather than prism) isomer was identified as the lowest-energy isomer from highly accurate rotation−vibration tunneling (VRT) spectroscopy near 5 K,[3,4] which should be attributed to zero-point-energy and/or entropic effects modifying the stability order. Thus, the above isomers are very close energetically, rendering their identification challenging. Further VRT experiments observed also the prism and book isomers.[5]

A commonly utilized experimental method is vibrational IR spectroscopy in solid matrices,[6−9] liquid helium,[10,11] or gas-phase molecular beams.[12−15] The solid matrices and liquid helium experiments can achieve very low temperatures, but with no mass selection, so that both the cluster size and its isomeric form have to be assigned. The molecular beam experiments achieve mass selection, but the vibrational temperature is not well defined. The picture that emerges is rather confusing. For water in liquid He, one IR band was attributed to the ring isomer, dubbed "the smallest piece of ice".[10] This was verified in solid *para*-$H_2$, in which a book isomer band was also observed, but mistakenly assigned to the cage.[7] In solid Ar and Kr, cage and book isomers were identified.[8] In contrast, gas-phase molecular beam studies assigned their spectra exclusively to the book isomer,[13,14] though a decade later, one of the authors retracted this assignment.[15]

The isomer identifications in the literature were based on the HBed OH stretching modes (3100−3700 cm$^{-1}$). There are six such modes for the ring, seven for the book, eight for the cage, and nine for the prism isomer, but only few of them are seen experimentally. Assignments relied heavily on theory, particularly on scaled harmonic frequencies from quantum chemistry calculations, such as density functional theory (DFT)[16] or wavefunction methods at the Møller−Plesset (MP2) level[17−20] or higher. Most accurate is coupled clusters with single, double, and triple excitations, CCSD(T).[20,21] Also,

**Received:** June 18, 2020
**Revised:** September 1, 2020
**Published:** September 1, 2020




https://dx.doi.org/10.1021/acs.jpca.0c05557
*J. Phys. Chem. A* 2020, 124, 8201−8208

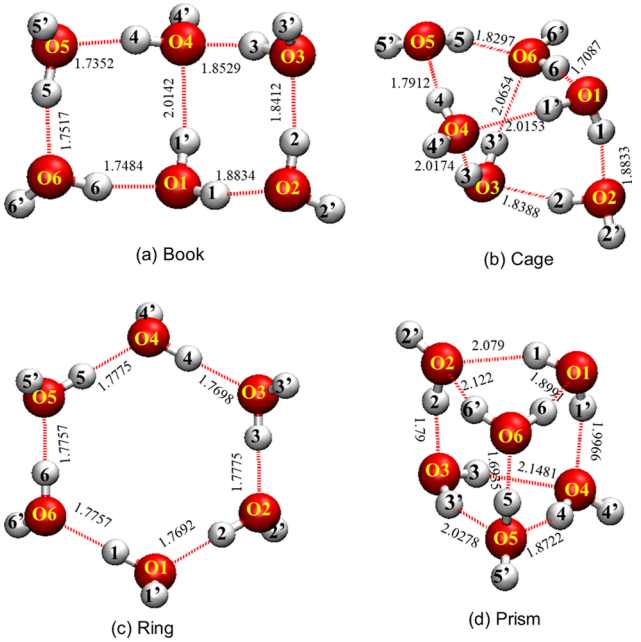


**Figure 1.** Structure of the four low-lying isomers of the water hexamer, with atom labels and the average HB lengths (in Å) during the 10 ns MB-pol trajectories at 10 K. For better visibility, the abbreviations $k$ and $k'$ are used for H$k$ (HBed H-atom number $k$) and H$k'$, respectively. Starting with the book isomer, the cage can be formed by adding the H3′···O6 HB, whereas the prism can be formed by adding the H3′···O5 and H6′···O2 HBs. In our notation, all non-HBed H atoms are of the H$k'$ type (plus some HBed ones).

anharmonic calculations were performed using vibrational second-order perturbation theory (VPT2).[19] These methods do not take into account finite-temperature effects.

Temperature effects are readily studied using molecular dynamics (MD). Recently, many-body (MB) analytical potential energy surfaces (PES) have been developed for water−water interactions.[22] These were parameterized against high-level CCSD(T) results. MB-PESs applied to the water hexamer include the explicit three-body (E3B2) PES from the Skinner group,[23,24] the WHBB PES from the Bowman group,[25−27] and the MB-pol PES from the Paesani group.[28,29] These may be used for normal-mode analysis at 0 K, or for obtaining the temperature dependence with MD simulations. MD on the E3B2 PES[23] showed that the gas-phase hexamer spectrum at 60 K[14] originates from a mixture of the book and cage isomers. Quantum statistical mechanics on the MB-pol PES indeed found the book population increasing with $T$, at the expense of diminishing cage population.[29] In contrast, WHBB simulations found "very good agreement with the earlier molecular beam experiments of Buch, Buck, and co-workers[14] who, as it turns out, correctly interpreted their spectrum as the book isomer".[27]

The conflicting results may arise partly from deficiencies in the theoretical models for water. We estimate that for positive isomer identification, the maximal deviation (maxD) between the experimental and theoretical frequencies should be smaller than the smallest spacing between vibrational lines of a given isomer, ca. 20 $cm^{-1}$ (see tables below). Moreover, experimental bands from different isomers may sometimes be ∼10 $cm^{-1}$ apart (see book and cage isomers below); therefore, we also require that the mean absolute deviation (MAD) between theory and experiment be <10 $cm^{-1}$.

Table S1 in the Supporting Information (SI) shows that no previous MB-PES dynamics achieved such accuracy. With quantum chemistry, no DFT theory possesses such high resolution. For example, in comparing DFT harmonic frequencies from 34 density functionals with benchmark harmonic frequencies for the book isomer, all functionals gave maxD > 50 $cm^{-1}$, some deviating by 100's of $cm^{-1}$ (Table 1 of ref 16). With wavefunction methods, one can get maxD < 50 $cm^{-1}$ for harmonic frequencies only on the CCSD(T) level of computation (Figure 5 of ref 20). The computed frequencies are then 150−200 $cm^{-1}$ higher than the experimental due to the absence of anharmonicities. This is commonly corrected by an empirical scaling parameter, $\alpha$. Table S2 shows that optimally scaled harmonic frequencies sometimes obtain the above resolution and sometimes do not (depending, e.g., on the basis set). It would be desired to perform anharmonic calculations that do not require empirical correction factors, but Table S2 shows that VPT2 fairs rather poorly for the water hexamer.

We have recently utilized the MB-pol PES to calculate the vibrational spectra of the ring isomers of small water clusters, $W_{n=2-5}$, as a function of temperature.[30] One is restricted to classical dynamics because nuclear quantum dynamics at such low temperatures can generate equilibrium properties,[29] but not dynamic attributes such as vibrational spectra. Motivated by previous MB-pol simulations of liquid water,[31] we have demonstrated that velocity autocorrelation function (VACF) spectra for classical MB-pol trajectories of small water clusters can be accurately corrected for nuclear quantum effects (NQE) by subtracting a constant frequency (the "NQE shift").[30] This constant depends on the cluster size and isomer, but not on temperature or the vibrational mode within the HBed OH manifold.

Here, we show how shifting the classical MB-pol frequencies generates exceptionally accurate OH stretch spectra for the water hexamer. To avoid having an adjustable parameter for each isomer, we optimize the NQE shift in comparison to scaled harmonic CCSD(T) frequencies, using a single scaling parameter for all four isomers. The procedure produces excellent agreement with experiment that allows secure isomer identification and a first theoretical determination of their NQE shifts. We find that the NQE is large for the 2D clusters and decreases for the 3D clusters to values closer to that of liquid water (lw). The method also allows us to determine the temperature effect on the OH band frequencies of the cage isomer, in the temperature range where it is the dominant isomer of the water hexamer.

## ■ COMPUTATIONAL METHODS

Similar to our earlier work,[30] all of the classical MD simulations have been performed using the MB-pol PES that has been built upon the many-body expansion of the interaction energy, which includes explicit expressions for one-body (1B), two-body (2B), and three-body (3B) interactions, along with classical N-body polarization to account for all higher-body contributions to the interaction energy.[28] MB-pol is publicly available on various platforms, e.g., as an external plugin for the OpenMM toolkit for molecular simulations. We have used the OpenMM platform to run classical MD, where atom positions and velocities are propagated in time using Newton's laws, with the forces obtained by differentiation of the analytic MB-pol potential.


https://dx.doi.org/10.1021/acs.jpca.0c05557
J. Phys. Chem. A 2020, 124, 8201−8208

Four hexamer isomers have been studied (book, cage, ring, and prism). Their initial configurations were optimized at the B3LYP-D3/6-311++G** level of theory using the Gaussian 09 software (http://gaussian.com/glossary/g09/). Starting from the optimized structures, we ran 10 ns NVT trajectories (constant number of particles, volume, and temperature) at 10 K, using the g-BAOAB integrator. The first 0.2 ns was considered as equilibration and excluded from the analysis. In addition to the accurate integrator, we also used a small time step, 0.2 fs, with coordinates saved every 1 fs for spectral analysis. For the temperature effect, we started with the optimized book structure and ran NVT simulations at 30, 50, and 70 K. The initial conformation converted rapidly to the cage structure, which is therefore the only isomer for which we can get the temperature effect.

Vibrational spectra were calculated from the velocity autocorrelation function (VACF), first transformed into the frequency domain using discrete fast Fourier transform (FFT), then multiplied by its complex conjugate, and transformed back into the time domain using inverse FFT (iFFT) to obtain the VACF. A Gaussian window function was applied to suppress noise in the VACF, and the result was again Fourier-transformed to produce the spectrum. We already noted,[30] using DFT methods, that in the absence of a dipole surface, vibrational intensities are usually not correct, but the frequencies are very accurate (within 0−2 $cm^{-1}$ of the dipole autocorrelation frequencies). Here, we have calculated two kinds of VACFs: an all H-atom VACF, based on the velocity autocorrelation of all H atoms (i.e., excluding the heavy oxygens), and partial VACFs that are based on autocorrelating specific OH bonds. For decoupled OH bands, the latter identifies the OH oscillator giving rise to a specific band, termed here "local mode assignment" (LMA). For coupled OH stretches, the partial VACF helps identify the OH bonds contributing at each normal-mode frequency.

## RESULTS

**Book Isomer.** We begin with the book isomer, for which one has the most detailed experimental spectrum,[13] previously assigned using scaled MP2 harmonic frequencies.[17] Its structure is shown in Figure 1a, which also introduces the atom labeling nomenclator. Figure 2a shows its VACF spectrum at 10 K from all of the H atoms in the cluster, obtained from classical MD simulations using the MB-pol PES (no NQE correction yet). Figure 2b shows the (partial) VACF of the individual OH distances. This helps in assigning the bands to individual OH stretches and assessing the extent of their couplings.

$W_6$ has 12 OH oscillators, hence 12 stretching modes, labeled 1−12. In the book isomer, these modes are assigned as follows. Modes 1−4 are "free" (not HBed) OH stretches of the four water molecules not participating in the O1H1′···O4 bridge. Mode 5 involves the free OH on O4. The HBed OH modes discussed herein are thus modes 6−12. There are two approaches for assigning them: as either local or normal modes.

In the LMA, each band is assigned to the OH bond that makes the dominant contribution to its intensity. In addition, one notes the HBing pattern of the O atom as an HB donor. Thus, O*k*H*k*(DAA) means that oxygen O*k* donates an HB through hydrogen atom H*k* when, in addition, it accepts two HBs. The LMA is given in the figure legend and, as common in water clusters,[32] the most red-shifted HBed OH stretch is of the DAA type, the least red-shifted are of the DDA type, while DA oxygens are in-between. This may be ascribed to the water cooperativity effect: accepting HBs strengthens the donor capabilities (thus weakening the O*k*H*k* bond), whereas donating an additional HB weakens the donor capabilities. A single DDA oxygen atom (here, O1) is responsible for two modes, the weakest being O1H1′(DDA) (mode 6) that is the bridging moiety. A comparison with the HB distances in Figure 1a shows a good correlation with the OH frequencies (short HB—red-shifted OH band). This analysis is in good agreement with previous results for the book isomer,[14] except for the relative order of O3H3(DA) and O1H1(DDA), i.e., modes 7 and 8, which are close in frequency and hence tend to mix.

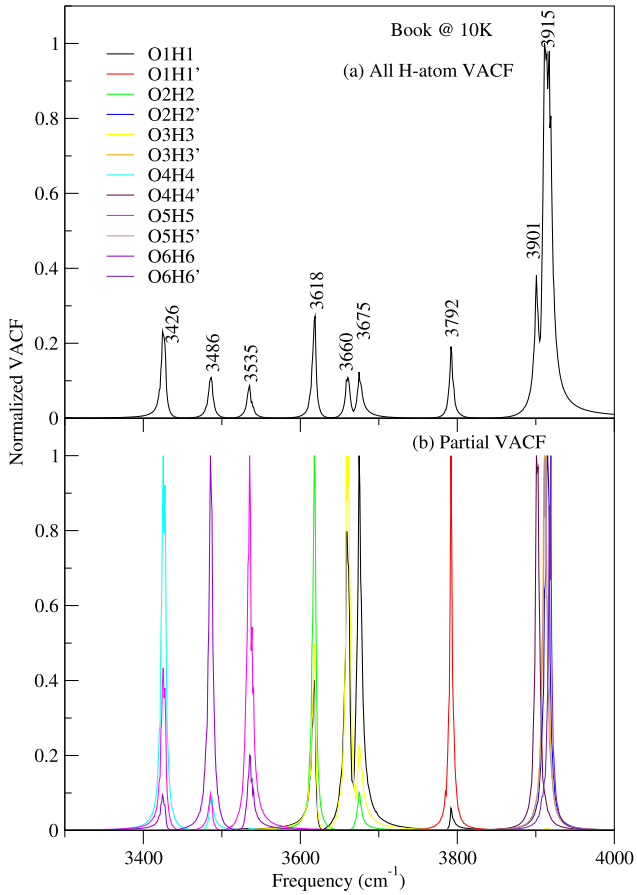


**Figure 2.** VACF vibrational spectra of the book isomer of the water hexamer (without NQE correction), from a 10 ns MB-pol simulation at 10 K. (a) All H-atom VACF spectrum with peak frequencies marked (in $cm^{-1}$). (b) Partial VACF spectra for the 12 OH oscillators, each coded in a different color. The LMA of the HBed OH stretches can be read from this figure as follows (low to high): O4H4 (DAA), O6H6 (DA), O5H5 (DA), O2H2(DA), O3H3 (DA), O1H1 (DDA), O1H1′(DDA).

Less attention was offered in the literature to the normal modes, which arise when local modes are close in energy, have the same symmetry, and mix together. This is seen in Figure 2b, with more than one OH oscillator contributing intensity at a given frequency. Modes 7−12 can be divided into two groups. Modes 7, 8, and 9 are due to the HBed OH oscillators O1H1, O2H2, and O3H3, in the O1−O2−O3−O4 ring, which are orientated contra O1H1′ (anticooperativity). Hence, these three oscillators participate in weak HBs, and their


https://dx.doi.org/10.1021/acs.jpca.0c05557
J. Phys. Chem. A 2020, 124, 8201−8208

frequencies are the least red-shifted. Modes 10, 11, and 12 are the HBed OH oscillators in the "tetrameric" ring, O1−O4−O5−O6. In this ring, the HBs are short because O4H4, O5H5, and O6H6 have the same orientation as O1H1′ (water cooperativity effect). Hence, their frequencies are the most red-shifted. This explains the relative positions of the four DA modes, splitting into two groups between the DAA and DDA bands. Additionally, Figure 2 shows that the three modes in each tetrameric ring are coupled, but there are no couplings between rings.

To determine the NQE shift, we compare the MB-pol and CCSD(T) frequencies, which we denote by $f_i$ and $g_i$, respectively. These frequencies are corrected by shifting and scaling, respectively. The scaling factor, $\alpha$, corrects for the lack of anharmonicity in the quantal frequencies, while the NQE shift corrects for the lack of NQE in classical MD. After these corrections, we expect to obtain the same frequencies, $f_i - \mathrm{NQE} = \alpha g_i$, at least on average:

$$\mathrm{NQE} = \sum_{i=1}^{m} (f_i - \alpha g_i)/m \tag{1}$$

The averaging here is over the $m$ HBed OH modes. The scaling factor, $\alpha$, is assumed to possess the same value for all isomers, so we determine it for the book isomer, as the average ratio of the experimental[13] and computed CCSD(T):MP2 frequencies.[20] The latter utilized the haQZ basis set (Dunning's cc-pVQZ basis set augmented with diffuse functions on all nonhydrogen atoms), close to the complete basis set (CBS) limit.

For comparison with the gas-phase measurements,[13] the 12 theoretical OH stretching modes are assumed to generate seven bands as follows. Modes 1−4 average to the single free OH band. The $O_4H_4'$ stretch (mode 5) is not seen experimentally as a separate band. Modes 7 and 8 coalesce into a single experimental band, which is compared with the average of the two theoretical bands. Additionally, the red-most experimental band (3169 $cm^{-1}$) was identified as the water monomer bending overtone,[27] and is thus excluded from our analysis. This is crucial for correctly aligning the experimental and theoretical bands.

With these assumptions, one obtains $\alpha$ = 0.950 for the CCSD(T) harmonic spectrum, and subsequently, from eq 1, NQE = 208 $cm^{-1}$ for the book hexamer. For the remaining three isomers, we will assume that $\alpha$ is constant (namely, in contrast to the NQE, it is not isomeric sensitive). Thus, the remaining spectra will be obtained with no new adjustable parameters.

For the book isomer, the shifted MB-pol and scaled CCSD(T) frequencies show a similarly good agreement with experiment (Table 1). Both have MAD < 10 $cm^{-1}$ and maxD < 20 $cm^{-1}$, which is the accuracy limit that, from our experience, is necessary for unequivocal assignments. Therefore, we can conclude that the gas-phase measurements with which we are comparing[13] are indeed of a pure book isomer, as found for the WHBB potential.[27]

Two frequencies are also available from 25 K argon matrix experiments.[8] The band at 3215 $cm^{-1}$ is in good agreement with the MB-pol frequency of mode 12 at 10 K. However, the gas-phase experiment of Diken et al. shows a notably red-shifted band, at 3201 $cm^{-1}$. While the experimental temperature was not reported in this study,[13] it was generally assumed to be 50−100 K.[23] As will now be demonstrated for the cage isomer, a red shift is induced by lowering $T$, suggesting that the vibrational temperature in the Diken experiment was actually below that of the 25 K matrix.

**Table 1. OH Stretch Frequencies (in $cm^{-1}$) for the Book Isomer of the Water Hexamer: Experiment vs Shifted MB-pol and Scaled Harmonic CCSD(T) Calculations**

| mode | gas[a] | gas,[b] 60 K | matrix,[c] 25 K | MB-pol,[d] 10 K | CCSD(T)/haQZ[e] |
|---|---|---|---|---|---|
| 1−4 | 3711 | 3720 | | 3707 | 3705 |
| 5 | | | | 3693 | 3698 |
| 6 | 3572 | 3568 | | 3584 | 3580 |
| 7 | 3464 | 3451 | 3451 | 3467 | 3468 |
| 8 | | | | 3452 | 3455 |
| 9 | 3423 | 3400 | | 3410 | 3408 |
| 10 | 3327 | 3320 | | 3327 | 3328 |
| 11 | 3287 | 3283 | | 3278 | 3282 |
| 12 | 3201 | 3192 | 3215 | 3218 | 3217 |
| MAD | 0 | 10 | 13.5 | 8.5 | 7.8 |
| maxD | 0 | 23 | 14 | 17 | 16 |

[a]Molecular beam experiment, Table 1 of ref 13. MAD and maxD measured relative to this experiment. The band at 3169 $cm^{-1}$ was identified as bend overtone; hence, it is excluded from our analysis. [b]Molecular beam experiment, Exp(1) in Table 2 of ref 14. [c]Argon matrix experiment, Table 2 of ref 8. [d]This work, NQE shift of 208 $cm^{-1}$. MB-pol results at higher $T$ are not available because the cluster converts to the cage isomer. [e]Table S78 of ref 20, scaled by 0.950.

**Comparison with Other Methods.** Before proceeding to the other $W_6$ isomers, it is instructive to compare our results for the book isomer with some previously published results (Tables S1−S3). First, consider the MB-PES results (Table S1): Can they also benefit from introducing a constant shift for the HBed OH stretching frequencies? To answer this question, we included in Table S1 also the mean deviation (meanD), defined as $\sum_{i=1}^{m}(f_i - e_i)/m$, where $e_i$ are the experimental frequencies and $f_i$ are those calculated from the dynamical method. Evidently, meanD = 0 does not imply a good fit ($f_i = e_i$) because there may be large errors of opposite signs that cancel each other. Hence, we routinely use the

$$\mathrm{MAD} \equiv \sum_{i=1}^{m} |f_i - e_i|/m$$

criterion instead. The MAD can vanish only when all $f_i = e_i$. Now, if meanD = 0, whereas MAD is large, it is not possible to improve the fit by a constant shift. For example, if we add to all frequencies a constant $f_0$, then we will get meanD = $f_0$, which just worsens the fit.

Table S1 shows that for the WHBB[27] and MBpol/LM[29] methods, meanD is small. Thus, in these cases, a constant shift can improve the fit only marginally. Indeed, these calculations already take into account the quantal nature of the nuclei, so they are not expected to benefit from NQE corrections. For the E3B2 results,[24] both MAD and meanD are large (in absolute value). Here, we find that shifting reduces the error by half, but the remaining error is still large compared to our shifted MB-pol frequencies. The observation that introducing a constant shift resurrects only classical results on the most accurate PES supports its utilization as an NQE correction.

Next, consider the NQE shifts obtained using one of the quantum chemistry calculations in Table S2, instead of CCSD(T) that was utilized in Table 1. Interestingly, all of these have meanD($g$) $\equiv \sum_{i=1}^{m}(\alpha g_i - e_i)/m \approx 0$, namely, error cancellation over the OH stretch manifold, where $g_i$ are the


https://dx.doi.org/10.1021/acs.jpca.0c05557
J. Phys. Chem. A 2020, 124, 8201−8208

frequencies calculated by a quantum chemistry method and $\alpha$ is their scaling factor. Rewriting eq 1 as

$$\mathrm{NQE} = \sum_{i=1}^{m} [(f_i - e_i) + (e_i - \alpha g_i)]/m$$
$$= \mathrm{meanD}(f) - \mathrm{meanD}(g) \quad (2)$$

shows that if meanD($g$) = 0, the NQE is independent of $g_i$, namely, independent of the ab initio reference method. This is demonstrated in Table S3, which shows that (in spite of the large differences in their MAD), the three ab initio calculations produce nearly identical NQE shifts.

Thus, determining the NQE shift from MB-pol simulations does not necessarily require a high-level quantum computation as a reference, provided that the latter has near-zero mean with respect to the experimental frequencies of the group of modes under consideration. Stated differently, a scaled quantum harmonic calculation can be completely useless in assigning the IR spectrum (when it exhibits a large MAD), but if it has meanD = 0, it can still be used to shift the MB-pol frequencies to best-fit experiment.

**Cage Isomer.** This is the most stable isomer for the MB-pol water hexamer at low temperatures,[29,33] in agreement with experiment.[3] Its 10 K classical MB-pol VACF spectrum is shown in Figure S1 of the SI. Similar to the book isomer in Figure 2b, Figure S1b shows the LMA for the cage isomer from partial VACFs, again noting that the DAA water molecules (O4 and O6) have the most red-shifted OH modes, whereas the DDA oxygen atoms (O1 and O3) are the least red-shifted. O1 and O3 donate two HBs each: the O1H1′ and O3H3′ hydroxyls, participating in the two HBs bridging over the ring isomer structure, are the least red-shifted within the DDA group. The DA moieties are in-between the DAA and DDA limits.

To obtain the NQE shift for the cage isomer, 202 cm$^{-1}$, we utilize the harmonic CCSD(T):MP2 frequencies,[20] while retaining, in eq 1, $\alpha$ = 0.950 as obtained for the book isomer. Consequently, there are no new adjustable parameters for comparing with experiment. Table 2 compares the scaled CCSD(T) and shifted MB-pol frequencies with experiments in Ar matrices (25 K).[8] The shifted MB-pol frequencies at 10 K are in somewhat worse agreement with experiment compared with the book isomer in Table 1, particularly for mode 12, which is blue-shifted with respect to experiment. However, the experimental data are at 25 rather than 10 K, and hence we consider the temperature effect.

**Temperature Effect.** For the cage isomer, it is easy to obtain the temperature dependence because, as the temperature is raised above 10 K in the classical trajectories, all isomers rapidly convert to the cage isomer (our starting configuration was the book). Thus, we have simulated the cage at 30, 50, and 70 K. Its all H-atom VACF spectra are shown in Figure 3a, and the partial VACF spectra are shown in the SI (Figures S2–S4). For the dimer to pentamer series, we have previously shown[30] that the OH stretch NQE is temperature-independent within this temperature range. With this assumption, the MB-pol frequencies for 30, 50, and 70 K were obtained (Table 2).

**Table 2. OH Stretch Frequencies (in cm$^{-1}$) for the Cage Isomer of the Water Hexamer**

| mode | matrix,[a] 25 K | MB-pol,[b] 10 K | CCSD(T)/haQZ[c] | MB-pol,[b] 30 K | MB-pol,[b] 50 K | MB-pol,[b] 70 K |
|---|---|---|---|---|---|---|
| 1–4 | | 3716 | 3702 | 3708 | 3706 | 3706 |
| 5 | | 3607 | 3602 | 3609 | 3610 | 3614 |
| 6 | | 3569 | 3569 | 3571 | 3573 | 3573 |
| 7 | 3543 | 3538 | 3532 | 3537 | 3538 | 3539 |
| 8 | 3471 | 3474 | 3467 | 3478 | 3482 | 3483 |
| 9 | 3412 | 3418 | 3424 | 3425 | 3430 | 3437 |
| 10 | 3391 | 3365 | 3378 | 3371 | 3374 | 3379 |
| 11 | 3339 | 3333 | 3341 | 3344 | 3352 | 3358 |
| 12 | 3137 | 3113 | 3158 | 3123 | 3139 | 3149 |
| MAD | 0 | 11.6 | 10.3 | 10.8 | 11 | 14 |
| maxD | 0 | 24 | 20 | 20 | 18 | 25 |

[a]Experiments on water in Ar matrix, from Table 2 of ref 8. MAD and maxD relative to these data. [b]This work, Figures S1–S4 with an NQE shift of 202 cm$^{-1}$. [c]Table S81 of ref 20, scaled by 0.950.

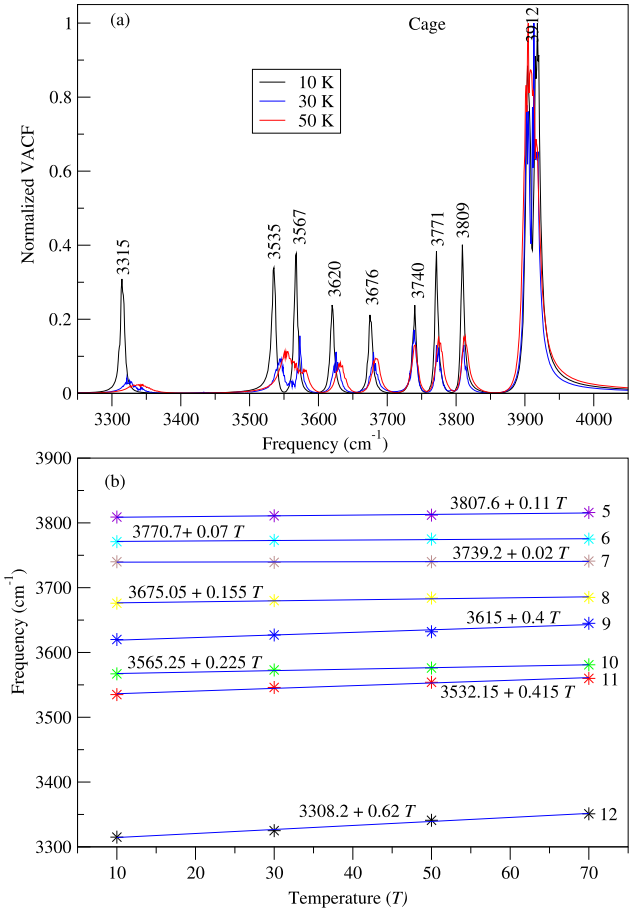


**Figure 3.** Vibrational spectroscopy of the water hexamer cage isomer from a classical 10 ns MB-pol simulation. (a) All H-atom VACF spectra at 10, 30, and 50 K. (b) Temperature dependence of the HBed OH peak frequencies for the eight HBed OH modes. Lines are linear fits, with the fitting equation adjacent to each line. To correct the frequencies for NQE, subtract 202 cm$^{-1}$.

The width of all bands increases with increasing $T$ to the extent that, for $T$ > 50 K, modes 10 and 11 overlap to yield a single wide band. In addition, the band centers shift, with increasing $T$, in opposite directions for the free and HBed OH modes. While the free OH bands show a small red shift (apparently sampling more anharmonic regions of the potential at higher energies), the HBed OH bands (excepting mode 7) all blue-shift (Figure 3b). In agreement with our


https://dx.doi.org/10.1021/acs.jpca.0c05557
J. Phys. Chem. A 2020, 124, 8201–8208

previous work,[30] the largest blue-shift is observed for the most red-shifted band (here, mode 12). The 30 K simulation indeed generates better agreement with the 25 K experiment than the 10 K simulation, though this is true also at 50 K (Table 2).

Some remarks on the temperature dependence of the isomer distributions are warranted. In our classical simulations, the cage is the major isomer up to at least 70 K, as indicated by the absence of the low-frequency book isomer bands 11 and 12 in the spectrum shown in Figure 3a and by the straight lines in Figure 3b. Other isomers are seen only transiently, at 70 K. The quantum isomer distribution from the MB-pol potential, Figure 1b of ref 29, shows the cage population decreasing from 1 at 0 K to about 0.7 at 50 K. The transition from cage to book involves the cleavage of one weak HB cross-linking the two pages of the book. Cleavage of such a weak HB is enhanced in quantal calculations, when the zero-point energy supplies most of the required energy. This could explain why we see predominantly the cage isomer in this temperature range.

**Ring Isomer.** MB-pol spectra for the ring isomer are given in Figure S5 of the SI. In this case, all six water molecules are of the AD type. Due to symmetry, an LMA will predict a single mode. Indeed, our MB-pol calculations show that, compared to the other isomers, the six HBed OH modes fall here within a narrow frequency range of 98 $cm^{-1}$ (Table 3). Yet this range is not negligible. The splitting of the OH stretching bands is due to their strong coupling so that a normal-mode picture is essential for understanding the ring isomer. The optimized CCSD(T) structure has $S_6$ symmetry.[21] This high symmetry results in two doubly degenerate normal modes ($E_1$ and $E_2$), the four irreducible representations (A, $E_1$, $E_2$, and B) being isomorphic with those of the Hückel theory for benzene. In the MD, the symmetry is reduced so that the doubly degenerate modes split.

**Table 3. OH Stretch Frequencies (in $cm^{-1}$) for the Ring Isomer of the Water Hexamer**

| mode[a] | matrix[b] | MB-pol[c] | CCSD(T)[d] |
|---|---|---|---|
| 1−6 | | 3687 | 3706 |
| 7 (B) | | 3386 | 3391 |
| 8 ($E_2$) | | 3372 | 3376 |
| 9 ($E_2$) | | 3368 | 3376 |
| 10 ($E_1$) | 3335 | 3337 | 3330 |
| 11 ($E_1$) | 3319 | 3320 | 3330 |
| 12 (A) | | 3288 | 3268 |

[a]Symmetry type in parentheses. [b]3335 $cm^{-1}$ in liquid He,[11] 3319 $cm^{-1}$ in solid *para*-$H_2$.[7] [c]This work, NQE shift of 235 $cm^{-1}$. [d]Table S75 of ref 20, scaled by 0.950.

Experimental frequencies were reported for the IR-active $E_1$ mode in either liquid He or a *para*-$H_2$ matrix.[7,10] Scaling the CCSD(T):MP2 frequencies[20] by $\alpha$ = 0.95, as determined above for the book isomer, we obtain from eq 1 an NQE of 235 $cm^{-1}$, the largest value found thus far. This appears to correlate with the exceptionally large couplings in the ring isomer, the only isomer in which all HBed OH oscillators are coupled. Table 3 shows that, with no new adjustable parameters, the agreement of both calculations with experiment is better than the difference between the experimental frequencies in the two environments. In the present case, however, the optimal NQE shift for the HBed modes is not optimal for the free OH modes. Thus, each class of vibrational modes (free OH, HBed OH, bends, etc.) is characterized by their own NQE shift.

**Prism Isomer.** This isomer occupies the lowest potential energy well on the MB-pol PES, but is higher in free energy than the cage isomer.[29,33] It has been observed in VRT experiments.[5] The MB-pol spectra for the prism isomer are shown in Figure S6 of the SI. Here, all of the water molecules are either of the DAA (four low-frequency modes) or DDA (five high-frequency modes) type. They all have a coordination number of 3, which is the closest to that of lw.

As above, we determined the optimal shift parameter for this isomer by comparison with the scaled CCSD(T):MP2 frequencies[20] for its nine HBed OH bands (eq 1). The NQE here is 194 $cm^{-1}$, the smallest found thus far for the hexamer. The NQE-shifted frequencies are presented in Table 4.

**Table 4. OH Stretch Frequencies (in $cm^{-1}$) for the Prism Isomer of the Water Hexamer**

| mode | MB-pol[a] | CCSD(T)[b] |
|---|---|---|
| 1−3 | 3719 | 3704 |
| 4 | 3630 | 3630 |
| 5 | 3617 | 3609 |
| 6 | 3601 | 3595 |
| 7 | 3558 | 3548 |
| 8 | 3539 | 3531 |
| 9 | 3437 | 3439 |
| 10 | 3413 | 3421 |
| 11 | 3325 | 3334 |
| 12 | 3120 | 3136 |

[a]This work, NQE shift of 194 $cm^{-1}$. [b]Table S84 of ref 20, scaled by 0.950.

## CONCLUSIONS

In this work, we have demonstrated, for the water hexamer, a simple procedure for determining the NQE on its HBed OH stretching bands. This, in turn, allows one to introduce temperature effects extending the high-level quantum calculations to finite *T*. At 0 K, the experimental OH frequencies are accurately described by either scaled quantum harmonic frequencies or shifted classical MB-pol frequencies. The scaling factor, common to all isomers, was determined once for the book isomer. The isomer-dependent NQE shift was subsequently determined by demanding that, on average, the two frequencies coincide (eq 1).

The NQE shifts for the four hexamer isomers are summarized in Table 5. Their accuracy is corroborated by the close agreement demonstrated with experimental results,

**Table 5. NQE Shifts for MB-pol Isomers of the Water Hexamer (See Graphical TOC Entry)**

| isomer | # HBs[a] | NQE[b] ($cm^{-1}$) | $\nu_{12}$[c] ($cm^{-1}$) |
|---|---|---|---|
| prism | 9 | 194 | 3120 |
| cage | 8 | 202 | 3113 |
| book | 7 | 208 | 3218 |
| ring | 6 | 235 | 3288 |

[a]Number of HBs in the cluster. [b]NQE shifts determined from classical MB-pol HBed OH frequencies and CCSD(T) harmonic frequencies via eq 1. [c]Frequency of the most red-shifted OH band (mode 12) at 10 K.



https://dx.doi.org/10.1021/acs.jpca.0c05557
J. Phys. Chem. A 2020, 124, 8201−8208

whenever these exist. With increasing number of HBs in the cluster (a more 3D structure), the NQE decreases (see also Graphical TOC Entry). The behavior is nearly linear, excepting the ring that has an unusually high NQE. In contrast, $\nu_{12}$ does not show such a regular dependence with the number of HBs. However, it is the most sensitive to dimensionality, showing larger red-shifts for the 3D clusters (prism and cage) as compared with the 2D clusters (ring and book).

The book and the ring isomers are the two planar ring systems of the water hexamer, whose NQE shifts can be compared to those of the smaller rings, $W_n$, $n$ = 2−5, determined in our previous investigations.[30] Table 6 shows

**Table 6. NQE Shifts (in $cm^{-1}$) for MB-pol Ring-like Water Clusters, $W_n$ ($n$ = 2−6), and Bulk Water and Ice**

| $n$[a] | NQE | ΔNQE[b] |
|---|---|---|
| lw[c] | 175 | |
| 2 | 175 | |
| 3 | 174 | 0 |
| 4 | 188 | 14 |
| 5 | 204 | 16 |
| ice[d] | 213 | |
| 6[e] | 222 | 18 |

[a] $n$ = 2, 3, 4, and 5 from our previous work.[30] [b] NQE($n$) − NQE($n$ − 1). [c] liquid water.[31] [d] bulk ice.[34] [e] [NQE(ring) + NQE(book)]/2.

that the trend of a nearly linearly increasing NQE with $n$ continues for the hexamer, provided that its NQE is represented by the average NQEs of the ring and book isomers. Thus, this table shows that the NQE increases with increasing size of the 2D water cluster. However, once the structure folds, becoming more 3D, its NQE decreases (Table 5). The minimal NQE (for $n$ = 2 and 3) is identical to that of lw, but the maximal NQE exceeds that of bulk ice, perhaps because the latter is not a truly 2D system.

The excess NQE (above that of lw) correlates, qualitatively at least, with the degree of coupling between the local modes as revealed by our partial VACF spectra at 10 K for the individual OH bonds. The ring isomer is the most extensively coupled (Figure S5b), followed by the book (Figure 2b). In these 2D cases, a normal-mode analysis is required for understanding the OH stretch spectra, and the NQE shifts are large. There are less couplings in the prism isomer (Figure S6b) and almost none for the cage (Figure S1b). The LMA is a better description for these 3D cases, and their excess NQE shifts are small in comparison to the 2D clusters.

Because the NQE shift is temperature-independent at low temperatures,[30] once it is established at 0 K, classical MB-pol trajectories can be corrected for NQE also for $T$ > 0 K. In agreement with previous work,[30,35] we find that, for the dominant cage isomer, the HBed OH bands broaden and blue-shift with increasing $T$. The largest shift occurs for $\nu_{12}$ and, since it is relatively isolated from the other bands, the extent of its blue shift could be used as a "thermometer" for the internal vibrational temperature of the cluster. Finally, MB PESs for halides in water have recently become available.[36] Perhaps simple methods as introduced herein could be useful in understanding nuclear quantum effects on aqueous ion solvation.

## ■ ASSOCIATED CONTENT

### Supporting Information

The Supporting Information is available free of charge at https://pubs.acs.org/doi/10.1021/acs.jpca.0c05557.

Other theories for the book isomer (Tables S1−S3); VACF spectra from MB-pol trajectories (Figures S1−S6)

## ■ AUTHOR INFORMATION


### Corresponding Author

**Noam Agmon** − *The Fritz Haber Research Center, Institute of Chemistry, The Hebrew University of Jerusalem, Jerusalem 9190401, Israel;* orcid.org/0000-0003-4339-8664; Email: agmon@fh.huji.ac.il

### Author

**Nagaprasad Reddy Samala** − *The Fritz Haber Research Center, Institute of Chemistry, The Hebrew University of Jerusalem, Jerusalem 9190401, Israel;* orcid.org/0000-0003-3427-8513

Complete contact information is available at: https://pubs.acs.org/10.1021/acs.jpca.0c05557


### Notes

The authors declare no competing financial interest.

## ■ ACKNOWLEDGMENTS

This study was supported by Israel Science Foundation grant 722/19. The Fritz Haber Research Center is supported by the Minerva Gesellschaft für die Forschung, München, FRG.

## ■ REFERENCES


(1) Saykally, R. J.; Wales, D. J. Pinning Down the Water Hexamer. *Science* **2012**, *336*, 814−815.

(2) Miliordos, E.; Xantheas, S. S. An Accurate and Efficient Computational Protocol for Obtaining the Complete Basis Set Limits of the Binding Energies of Water Clusters at the MP2 and CCSD(T) Levels of Theory: Application to $(H_2O)_m$, $m$ = 2−6, 8, 11, 16, and 17. *J. Chem. Phys.* **2015**, *142*, No. 234303.

(3) Liu, K.; Brown, M. G.; Carter, C.; Saykally, R. J.; Gregory, J. K.; Clary, D. C. Characterization of a Cage Form of the Water Hexamer. *Nature* **1996**, *381*, 501−503.

(4) Liu, K.; Brown, M. G.; Saykally, R. J. Terahertz Laser Vibration-Rotation Tunneling Spectroscopy and Dipole Moment of a Cage Form of the Water Hexamer. *J. Phys. Chem. A* **1997**, *101*, 8995−9010.

(5) Pérez, C.; Muckle, M. T.; Zaleski, D. P.; Seifert, N. A.; Temelso, B.; Shields, G. C.; Kisiel, Z.; Pate, B. H. Structures of Cage, Prism, and Book Isomers of Water Hexamer from Broadband Rotational Spectroscopy. *Science* **2012**, *336*, 897−901.

(6) Bentwood, R. M.; Barnes, A. J.; Orville-Thomas, W. J. Studies of intermolecular interactions by matrix isolation vibrational spectroscopy: Self-association of water. *J. Mol. Spectrosc.* **1980**, *84*, 391−404.

(7) Fajardo, M. E.; Tam, S. Observation of the Cyclic Water Hexamer in Solid Parahydrogen. *J. Chem. Phys.* **2001**, *115*, 6807−6810.

(8) Hirabayashi, S.; Yamada, K. M. T. Infrared Spectra and Structure of Water Clusters Trapped in Argon and Krypton Matrices. *J. Mol. Struct.* **2006**, *795*, 78−83.

(9) Ceponkus, J.; Uvdal, P.; Nelander, B. Water Tetramer, Pentamer, and Hexamer in Inert Matrices. *J. Phys. Chem. A* **2012**, *116*, 4842−4850.

(10) Nauta, K.; Miller, R. E. Formation of Cyclic Water Hexamer in Liquid Helium: The Smallest Piece of Ice. *Science* **2000**, *287*, 293−295.

(11) Burnham, C. J.; Xantheas, S. S.; Miller, M. A.; Applegate, B. E.; Miller, R. E. The Formation of Cyclic Water Complexes by Sequential Ring Insertion: Experiment and Theory. *J. Chem. Phys.* **2002**, *117*, 1109.
(12) Paul, J. B.; Collier, C. P.; Saykally, R. J.; Scherer, J. J.; O'Keefe, A. Direct Measurement of Water Cluster Concentrations by Infrared Cavity Ringdown Laser Absorption Spectroscopy. *J. Phys. Chem. A* **1997**, *101*, 5211−5214.
(13) Diken, E. G.; Robertson, W. H.; Johnson, M. A. The Vibrational Spectrum of the Neutral $(H_2O)_6$ Precursor to the "Magic" $(H_2O)_6^-$ Cluster Anion by Argon-Mediated, Population-Modulated Electron Attachment Spectroscopy. *J. Phys. Chem. A* **2004**, *108*, 64−68.
(14) Steinbach, C.; Andersson, P.; Melzer, M.; Kazimirski, J. K.; Buck, U.; Buch, V. Detection of the Book Isomer From the OH-Stretch Spectroscopy of Size Selected Water Hexamers. *Phys. Chem. Chem. Phys.* **2004**, *6*, 3320−3324.
(15) Buck, U.; Pradzynski, C. C.; Zeuch, T.; Dieterich, J. M.; Hartke, B. A Size Resolved Investigation of Large Water Clusters. *Phys. Chem. Chem. Phys.* **2014**, *16*, 6859−6871.
(16) Howard, J. C.; Enyard, J. D.; Tschumper, G. S. Assessing the Accuracy of Some Popular DFT Methods for Computing Harmonic Vibrational Frequencies of Water Clusters. *J. Chem. Phys.* **2015**, *143*, No. 214103.
(17) Kim, J.; Kim, K. S. Structures, Binding Energies, and Spectra of Isoenergetic Water Hexamer Clusters: Extensive Ab Initio Studies. *J. Chem. Phys.* **1998**, *109*, 5886−5895.
(18) Losada, M.; Leutwyler, S. Water Hexamer Clusters: Structures, Energies, and Predicted Mid-Infrared Spectra. *J. Chem. Phys.* **2002**, *117*, 2003−2016.
(19) Temelso, B.; Archer, K. A.; Shields, G. C. Benchmark Structures and Binding Energies of Small Water Clusters with Anharmonicity Corrections. *J. Phys. Chem. A* **2011**, *115*, 12034−12046.
(20) Howard, J. C.; Tschumper, G. S. Benchmark Structures and Harmonic Vibrational Frequencies Near the CCSD(T) Complete Basis Set Limit for Small Water Clusters: $(H_2O)_{n = 2, 3, 4, 5, 6}$. *J. Chem. Theor. Comput.* **2015**, *11*, 2126−2136.
(21) Miliordos, E.; Aprà, E.; Xantheas, S. S. Optimal Geometries and Harmonic Vibrational Frequencies of the Global Minima of Water Clusters $(H_2O)_n$, $n = 2 - 6$, and Several Hexamer Local Minima at the CCSD(T) Level of Theory. *J. Chem. Phys.* **2013**, *139*, No. 114302.
(22) Cisneros, G. A.; Wikfeldt, K. T.; Ojamäe, L.; Lu, J.; Xu, Y.; Torabifard, H.; Bartók, A. P.; Csányi, G.; Molinero, V.; Paesani, F. Modeling Molecular Interactions in Water: From Pairwise to Many-Body Potential Energy Functions. *Chem. Rev.* **2016**, *116*, 7501−7528.
(23) Tainter, C. J.; Skinner, J. L. The Water Hexamer: Three-Body Interactions, Structures, Energetics, and OH-Stretch Spectroscopy at Finite Temperature. *J. Chem. Phys.* **2012**, *137*, No. 104304.
(24) Kananenka, A. A.; Skinner, J. L. Fermi Resonance in OH-Stretch Vibrational Spectroscopy of Liquid Water and the Water Hexamer. *J. Chem. Phys.* **2018**, *148*, No. 244107.
(25) Wang, Y.; Huang, X.; Shepler, B. C.; Braams, B. J.; Bowman, J. M. Flexible, *Ab Initio* Potential, and Dipole Moment Surfaces For Water. I. Tests and Applications for Clusters Up to the 22-mer. *J. Chem. Phys.* **2011**, *134*, No. 094509.
(26) Wang, Y.; Babin, V.; Bowman, J. M.; Paesani, F. The Water Hexamer: Cage, Prism, or Both. Full Dimensional Quantum Simulations Say Both. *J. Am. Chem. Soc.* **2012**, *134*, 11116−11119.
(27) Wang, Y.; Bowman, J. M. IR Spectra of the Water Hexamer: Theory, with Inclusion of the Monomer Bend Overtone, and Experiment Are in Agreement. *J. Phys. Chem. Lett.* **2013**, *4*, 1104−1108.
(28) Reddy, S. K.; Straight, S. C.; Bajaj, P.; Pham, C. H.; Riera, M.; Moberg, D. R.; Morales, M. A.; Knight, C.; Götz, A. W.; Paesani, F. On the Accuracy of the MB-pol Many-Body Potential for Water: Interaction Energies, Vibrational Frequencies, and Classical Thermodynamic and Dynamical Properties from Clusters to Liquid Water and Ice. *J. Chem. Phys.* **2016**, *145*, No. 194504.
(29) Brown, S. E.; Götz, A. W.; Cheng, X.; Steele, R. P.; Mandelshtam, V. A.; Paesani, F. Monitoring Water Clusters "Melt" Through Vibrational Spectroscopy. *J. Am. Chem. Soc.* **2017**, *139*, 7082−7088.
(30) Samala, N. R.; Agmon, N. Temperature Dependence of Intramolecular Vibrational Bands in Small Water Clusters. *J. Phys. Chem. B* **2019**, *123*, 9428−9442.
(31) Reddy, S. K.; Moberg, D. R.; Straight, S. C.; Paesani, F. Temperature-Dependent Vibrational Spectra and Structure of Liquid Water from Classical and Quantum Simulations with the MB-pol Potential Energy Function. *J. Chem. Phys.* **2017**, *147*, No. 244504.
(32) Yang, H.; Song, Y.; Chen, H. Stabilities, Vibrational States and Hydrogen Bond Characteristics of Water Clusters. *J. Clust. Sci.* **2016**, *27*, 775−789.
(33) Mallory, J. D.; Mandelshtam, V. A. Diffusion Monte Carlo Studies of MB-pol $(H_2O)_{2-6}$ and $(D_2O)_{2-6}$ Clusters: Structures and Binding Energies. *J. Chem. Phys.* **2016**, *145*, No. 064308.
(34) Moberg, D. R.; Straight, S. C.; Knight, C.; Paesani, F. Molecular Origin of the Vibrational Structure of Ice $I_h$. *J. Phys. Chem. Lett.* **2017**, *8*, 2579−2583.
(35) Kang, D.; Dai, J.; Hou, Y.; Yuan, J. Structure and Vibrational Spectra of Small Water Clusters from First Principles Simulations. *J. Chem. Phys.* **2010**, *133*, No. 014302.
(36) Paesani, F.; Bajaj, P.; Riera, M. Chemical Accuracy in Modeling Halide Ion Hydration from Many-Body Representations. *Adv. Phys. X* **2019**, *4*, No. 1631212.


https://dx.doi.org/10.1021/acs.jpca.0c05557
J. Phys. Chem. A 2020, 124, 8201−8208